Synthesis of Activated Carbon-Supported Catalysis Systems and Research for Electrocatalytic Performance on Wastewater Treatment

Yılmaz, Selman İlteriş
Vocational School of Technical Sciences, Biomedical Technology Program, Istanbul University-Cerrahpasa, Istanbul, TURKEY

Osman, Huseyn; Uğurlu, Mehmet[*+]
Department of Chemistry Faculty of Science, Muğla Sitki Kocman University, Muğla, TURKEY

Ali İmran, Vaizoğullar
Vocational School of Healthcare, Med Lab Program, Mugla Sıtkı Koçman University, Muğla, TURKEY

Chaudhary, Abdul Jabbar
College of Health, Medicine and Life Sciences, Department of Life Sciences, Division of Environmental Sciences,
Brunel University London, UK

ABSTRACT: *Electrochemical oxidation methods are simple, use very few extra reagents, and are both technically and economically viable technologies that can be used for the treatment of various industrial effluent streams including olive wastewater. The treatment is based on the direct anodic oxidation method in which the pollutants are adsorbed on the anode surface and then reduced by the electron transport reaction. In this study, the effect of different catalysts on the treatment of olive wastewater is carried out by using electrocatalytic methods. Initially,* TiO_2/AC, $V_2O_5/TiO_2/AC$, $WO_3/TiO_2/AC$, *and* $V_2O_5/WO_3/TiO_2/AC$ *catalysts were prepared by a sol-gel method. Then, the removal of different pollutants such as color, phenol, lignin, and Chemical Oxygen Demand (COD) was investigated by using different experimental electrochemical processes. In the electrocatalytic oxidation process, synthesized catalytic materials were used as particle electrodes (working electrodes) with the graphite electrodes in an electrochemical cell. The treatment process was optimized by investigating the effects of different parameters, for example, treatment time, catalyst type, catalyst amount (as solid/liquid ratio), voltage, the amount of supporting electrolyte (NaCl), and suspension's pH. The* $V_2O_5/TiO_2/AC$ *catalyst exhibited the highest percentage of removal under all experimental conditions, with a significant effect of voltage on the removal capacity observed (82.95% for lignin and 74.42% for COD). While the pH effect showed limited influence on the removal performance, higher yields were observed in acidic conditions. The electrocatalytic reaction involves various steps such as adsorption, nano adsorption, electrooxidation, and electrocatalytic oxidation. The individual effects of these steps were also investigated, resulting in percentage color removals of 25.58%, 51.72%, and 72.42%, respectively.*

---

* *To whom correspondence should be addressed.*
\+ *E-mail: mehmetu@mu.edu.tr*

1021-9986/2024/1/132-152 21/$/7.01

When the data were evaluated in terms of kinetics, it was seen that the data provide a first-degree agreement of over 90 % in all experimental parameters and the removal rate constants of low molecular weight substances may generally be higher than the others. Despite its significant lignin removal efficiency, the catalytic process mentioned above yielded lower values compared to other catalytic methods. Additionally, it was observed that the phenol concentration increased as a result of this process. This suggests that for the catalytic oxidation of olive wastewater effluent, the preliminary treatment using an electrocatalytic process is found to be more effective. The synergistic combination of these processes was more effective than the individual process.

KEYWORDS: *Activated carbon, Electrocatalytic, Olive wastewater, TiO_2, V_2O_5, WO_3.*

INTRODUCTION

Olive Mill Water (OMW), also known as olive black water, is dark-colored, foul-smelling, turbid, has high suspended solids content, high organic matter load, high phenolic substances, and is very difficult to treat. It is reported that most of the existing treatment processes are not effective for the removal of different pollutants from black water due to the toxicity and high concentration of different organic compounds [1]. Common techniques for removing pollutants from wastewater include ion exchange, adsorption, filtration, and electrolytic processes [2-4].

In some studies, it has been reported that phenol and organic compounds are removed at the rate of 81 % and 71 % by the adsorption of activated clay [5]. However, when lime is used as a coagulant, organic substances are significantly reduced and especially o-diphenols can be significantly removed [6]. *Meyssami* and *Kasaeian* (2005) air flotation treatment using chitosan [7]. *Kiril et al.* (2008) treatment of OMW after physicochemical treatment [8]. *Ginos et al.* (2006) reported that the chemical treatment with ferrous sulfate/cationic polyelectrolyte and lime/cationic polyelectrolyte can also be used for the treatment of black water effluent streams [9]. *Chedeville et al.* (2009) reported that the ozonation process can be used to remove 90 % of phenolic compounds from olive effluent streams [10]. In another study, in which olive black water was diluted and subjected to the electrolysis process, 90 % of Total Organic Carbon (TOC), and 99 % of total phenol were removed within 60 minutes [11]. The effects of various parameters, for example, the addition of hydrogen peroxide (H_2O_2), as an oxidant, Poly Aluminium Chloride (PAC), and the use of iron and aluminium electrodes were also investigated. The results showed that 62-86 % COD removal and approximately 99 % oil grease removal were removed under the optimum conditions [12].

The electrocoagulation process, using iron and aluminium electrodes, showed that 55 % lignin, 80 % phenol, 40 % COD, and 80 % color removal was achieved with the iron electrode; whereas, 49 % lignin, 70 % phenol, 35 % COD, and 90 % color removal was achieved with the aluminium electrode [13]. It has also been reported that both oxidation and Advanced Oxidation Processes (AOPs) can be used for the treatment of olive black water. It is reported that the complete removal of polyphenols can be achieved in the Fenton process [14]. *Michael et al.* (2014) investigated the combined use of chemical pretreatment (coagulation and flocculation) and photocatalytic solar Fenton method [15,16] for the treatment of olive black water in a pilot-scale study. It has been reported in the literature that the synergistic combination of different processes is a viable method for the treatment of black water containing high concentrations of organic pollution and inhibitory substances [17]. *Justino et al.* (2010) used oxidation and biological processes together for the treatment of black water and removed 80-99 % COD under the optimum conditions. It is seen that-2 polyphenols and 65 % COD removal are achieved. in addition, 64-85 % COD removal is achieved with pre-treated anaerobic treatment [18].

The use of various types of catalytic materials for the treatment of industrial effluent streams is growing. It is reported that TiO_2-SiO_2 oxides are the two most widely used catalysts in photoelectrolysis areas and show good performance in the removal of toxic and non-biodegradable pollutants, synthetic dyes, phenols, and benzenes [19] from various wastewater streams. In addition,

TiO_2 has certain abilities such as catalytic activity, external electric field, separation of light-causing electrons and TiO_2 holes [20]. Recently, it has been stated that TiO_2 can be effective in the oxidation reaction without an external light source to a certain extent and provide a synergistic contribution to oxidation [21]. In the study on the subject, electrocatalytic removal of acid orange 7 (AO7) dyestuff was investigated by using Granular Activated Carbon (GAC) supported TiO_2-SiO_2 oxide (TiO_2-SiO_2/GAC). *Kaur* and *Singh* (2007) obtained 95 % Chemical Oxygen Demand (COD) removal as a result of photocatalytic oxidation of reactive red 198 (RR198) dyestuff [22]. In another similar study, 37.8 % COD, 30.1 % Total Organic Carbon (TOC), and 76 % total phenol (TF) removals were achieved in the electrooxidation of pistachio wastewater [23]. In addition, more than 98 % color removal was obtained in the electrocatalytic *study* of *Uğurlu* (2018) [24]. TiO_2, WO_3, and V_2O_5 catalysts and reactive orange 122 (RO122) dyestuff [25]. However, it is thought that sufficient studies may be limited to defining the roles of TiO_2 in electrocatalytic oxidation in literature studies.

Activated Carbon (AC) is commonly used in the adsorption process to remove organic compounds and/or separate free chlorine from wastewater. Removing organic matter from wastewater prevents chlorine in the water from chemically reacting with acids and forming trihalomethanes, a known class of carcinogens. However, as with any water treatment method, AC may not be sufficient to remove all possible contaminants. It can be recommended to be used intensively in advanced treatment. It is not suitable to be used especially in waters with a high organic load such as olive black water. In addition, regeneration difficulties occur after a certain use. However, considering the size of the surface area, there are studies suggesting that it can be used as a supporting material. Apart from the use of activated carbon as an adsorbent, in recent years, catalytic removal studies have been found by bonding the semiconductors (TiO_2) with various adsorbent materials [26,27]. In particular, studies have been encountered in which catalysts can be obtained by loading semiconductor materials with catalytic effects. In the presented study, the catalytic active TiO_2/AC material which is a top product was synthesized by loading TiO_2 on the activated carbon surface under optimum conditions taking into account the previous studies [28].

The distinctive aspects of electrochemical oxidation methods are simple operation, no extra reagents, and cost-effective technology, which may be a better option for effluent treatment. Considering the direct anodic oxidation method, the pollutants are adsorbed on the anode surface and then reduced by the electron transport reaction. Conversely, in the case of the indirect oxidation mode, strong oxidizers such as hypochlorite, ozone and hydrogen peroxide can be regenerated by electrochemical means during electrolysis. All these realizations take place only on the electrode surface. In this case, the increase in yield may be limited. In the presented study, it is thought that the oxidation reaction is carried to all parts and its continuity by using the working electrode: in this respect, it is thought that the presented study makes important contributions to this field.

The main aim of this study is to synthesize, characterize and optimize the use of V_2O_5/TiO_2/AC, W_2O_5/TiO_2/AC, and W_2O_5/V_2O_5/TiO_2/AC catalysts for the removal of color, phenol, lignin and COD from OMW by using electrocatalytic oxidation processes.

EXPERIMENTAL SECTION

Chemicals

The chemicals used in all experimental studies and the sources from which they were supplied are briefly given below:

Activated carbon, Ammonium para tungstate [$(NH_4)_{10}H_2(W_2O_7)_6$, 98 %)] and Acetone (CH_3COCH_3, 99 %) were obtained from Sigma Aldrich. Titanium tetra isopropoxide ($Ti(OCH(CH_3)_2)_4$, 98 %), Ammonium Monovanadate (NH_4VO_3, 99 %), Hydrogen peroxide (H_2O_2, 35 %), pure ethanol (CH_3CH_2OH), Carbonate/tartrate reagent, Na_2CO_3 (sodium carbonate), sodium tartrate ($Na_2C_4H_2O_4$, 99.5 %), H_2SO_4, (95- 97 %), $HgSO_4$ (99 %), Ag_2SO_4 (99 %), $K_2Cr_2O_7$ (99.5 %) and NaOH (97 %) were obtained from Merck. HCl for pH adjustments was obtained from Riedel de Haen.

Wastewater samples were taken from the local olive oil production facility which is the production period from Muğla region and in the winter season the procedure and taken into sterile containers with certain storage conditions. The samples were taken to the laboratory and stored at +5 ^oC. Olive black water sample was diluted in certain proportions and used in all experimental studies since it contains high concentrations of organic compounds. The characteristics of olive mill wastewater used in this work are presented in Table 1.

Table 1: Physico-chemical characteristics of olive mill wastewaters sample

Parameters	Value
Colour	black
pH	5–6.6
COD (mg/L)	$6.12x10^5$
BOD (mg/L)	55.4
Polyphenol (mg/L)	8.0
Lignin (mg/L)	25.5
Density (25°C) (g/L)	0.96
Conductivity (μS/cm)	7065

Devices/Instruments

The devices used and their intended application is briefly given here. WiseStir MSH 20A model magnetic stirrer with heater for mixing. Binder dryer oven for drying processes. Nüve brand MF 140 model 6000Watt muffle furnace for calcination processes. Pasco brand SF9584A model power supply for electrocatalytic oxidation experiments. For spectrophotometric measurements, Shimadzu brand UV 1601 model spectrophotometer (in peak scanning). and Dr Hach Lange 2800 model spectrophotometer. For COD measurements, Dr. Lange Dr 200 model thermostat heater. WTW pH330i model digital pH meter for pH measurement processes. Jeol Jem 2100 model TEM device for TEM analysis. Jeol Jem 7600F model SEM device for SEM analysis. Bruker 08 Advance model X-ray diffractometer for XRD analysis. Micrometrics Gemini 2380 model BET measuring device for BET analysis.

Synthesis of catalysts

A brief description of the processes used for the synthesis of different catalysts to be used in preliminary experimental work is given below.

For the synthesis of catalysts to be used in preliminary experimental work. 120 g Titanium Tetraisopropoxide was added to 120 mL of 99.8% (v/v) ethanol. While the solution was stirred, 100g of granulated activated carbon (AC), 8 mL of distilled water and 0.8 mL of Acetone, as a stabilizer, were added. It was observed that TiO_2 was formed as a result of 3 h of stirring and this resultant material was divided into four equal parts. The first part of the material was dried at 80 ºC, cooled to room temperature and then calcined gradually. The product was labelled as TiO_2/AC. Then 2.19g of ammonium monovanadate and 30 mL of ethanol were added into the second part and the resultant mixture turned into a gel by stirring for 2 hours. This material was dried at 80°C and allowed to cool for calcination at room temperature. This material was labelled as V_2O_5/TiO_2/AC. The same procedure was used by adding 1.98g of ammonium paratungstate and 30mL of ethanol into the third part and the resultant product was labelled as WO_3/TiO_2/AC. Finally, 2.19g of ammonium monovanadate, 1.98 g of ammonium paratungstate and 30 mL of ethanol were added into the fourth part of the material and the mixture was stirred continuously for 2 h. After the mixture became gel, it was dried at 80 ºC and allowed to cool to room temperature before calcination. This product was labelled as $WO_3/V_2O_5/TiO_2$/AC respectively.

Calcination process

Granular activated carbon, which has adsorbed the catalytic material, was heated up to 300 ºC under nitrogen gas flow in the ash furnace (PLF Series 110-130. Protherm). The temperature was kept constant at 300 ºC for 1h and then the temperature was increased to 400 ºC and kept constant at 400 ºC for 1 h. The calcined products were then allowed to cool naturally to room temperature.

Electrocatalytic oxidation studies

All electrocatalytic oxidation experiments were carried out by adding Olive WasteWater (OWW) samples in the reactor with a volume of 300 mL using graphite electrodes (Fig. 1). To ensure adequate conductivity, 1 g/L of NaCl, as a supporting electrolyte, was added into the reactor and the mixing speed was kept constant for all experiments. Voltage (the electric charge potential difference between the two ends of the conductor in an electric current setup) was provided by graphite electrodes connected to an adjustable power supply. Electrocatalytic studies were carried out at room temperature (21 ºC) by keeping the mixing speed and the electrolyte (NaCl) amount constant. The degradation process was optimized by investigating the effects of catalyst type, change in voltage, solid/liquid ratio and suspension pH. The pH was adjusted with NaOH or HCl solution and monitored by using a pH meter equipped with a combined electrode. The changes in the concentration of color, phenol, lignin, and COD over time were analyzed according to standard wastewater analysis methods.

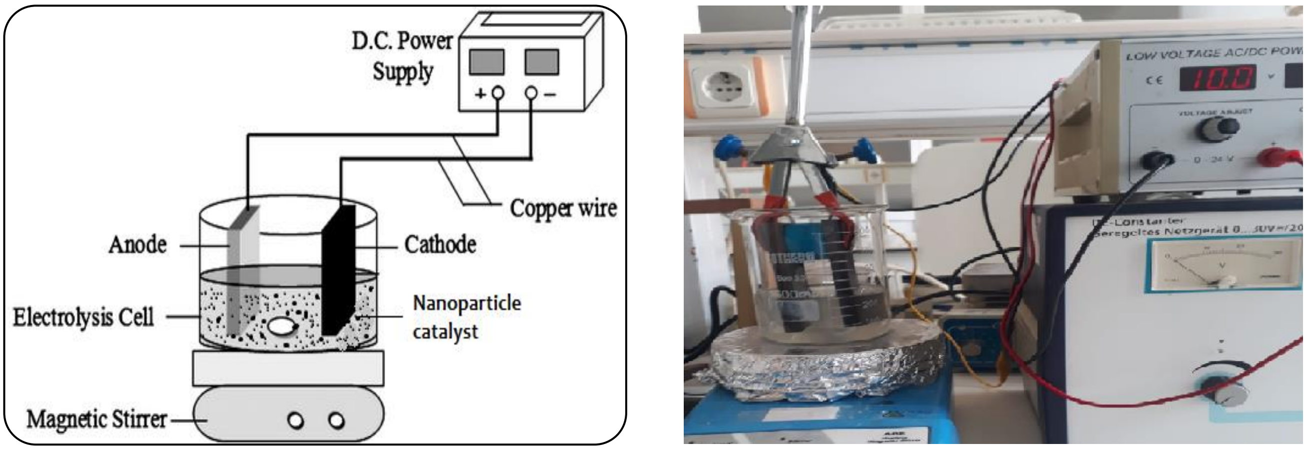

Fig. 1: Schematic view of the experimental setup used in electrocatalytic experiments

Analysis of Wastewater

Determination of color

The percentage removal of color was investigated by taking wastewater samples at different time intervals during the oxidation process. These samples were centrifuged and the liquid phase obtained was used to monitor the changes in the absorbance in the UV/visible region by using the spectrophotometric method. Based on the peak value observed at 400 nm wavelength (λ_{max} value = 400 nm), the changes in absorbance intensity according to the initial conditions were followed and the percentage removal was calculated according to the Eq. (1):

$$\text{Color removal (\%)} = \frac{A^{o}_{\lambda} - A_{\lambda}}{A^{o}_{\lambda}} \times 100 \qquad (1)$$

Here, A^{o}_{λ} refers to the initial absorbance and A_{λ} refers to the absorbance after the oxidation process.

Determination of lignin concentrations

Lignin concentration was determined by adding 0.2 mL of Folin-Ciocalteu reagent and 2 mL of carbonate-tartrate reagents to a 10 mL wastewater sample. The mixture was allowed to stand for 30 minutes for complex formation and then absorbance was measured at a wavelength of 700 nm. With the help of the calibration curve, the lignin concentrations were determined and the results were determined as the amount of substance that Folin-Ciocalteu reagent reduces [29].

Determination of COD amount

0.75 mL of digestion solution (potassium dichromate, mercury sulphate, sulfuric acid, water) and 1.75 mL of sulphate reagent (concentrated sulfuric acid, silver sulphate) were added in 1.25 mL of wastewater sample. The mixture was heated at 148 ºC using the thermostat heater for 2h. The COD concentration was determined colourimetrically using the UV-spectrophotometer at 600 nm [30].

Determination of phenol concentration

0.25 mL of 0.2 N ammonia solution was added to the 10 mL wastewater sample. The pH of the solution was adjusted to 7.9 ± 0.1 using a phosphate buffer prepared with sodium dihydrogen phosphate and disodium hydrogen phosphate. Then 0.1 mL of 2 % (m/v) 4-amino antipyrine and 0.1 mL potassium ferricyanide solutions were added, the mixture was allowed to stand for 15 min. for complex formation and finally, the absorbance was measured at 500 nm wavelength.

RESULTS AND DISCUSSION

Catalyst Characterization

Activated carbon and all the activated carbon-supported catalytic materials, e.g., TiO_2/AC, V_2O_5/TiO_2/AC, WO_3/TiO_2/AC, and WO_3/V_2O_5/TiO_2/AC were characterized by using Fourier Transform InfraRed (FT-IR) Spectrophotometer, Scanning Electron Microscope (SEM), Energy Dispersive X-ray (EDX), Transmission Electron Microscope (TEM) images, X-Ray Diffraction (XRD) spectra and Brunauer-Emmett-Teller (BET) for surface area measurements. The results obtained by using these analytical techniques are discussed below.

SEM analysis

SEM images of the used catalytic materials are shown in Fig. 2.

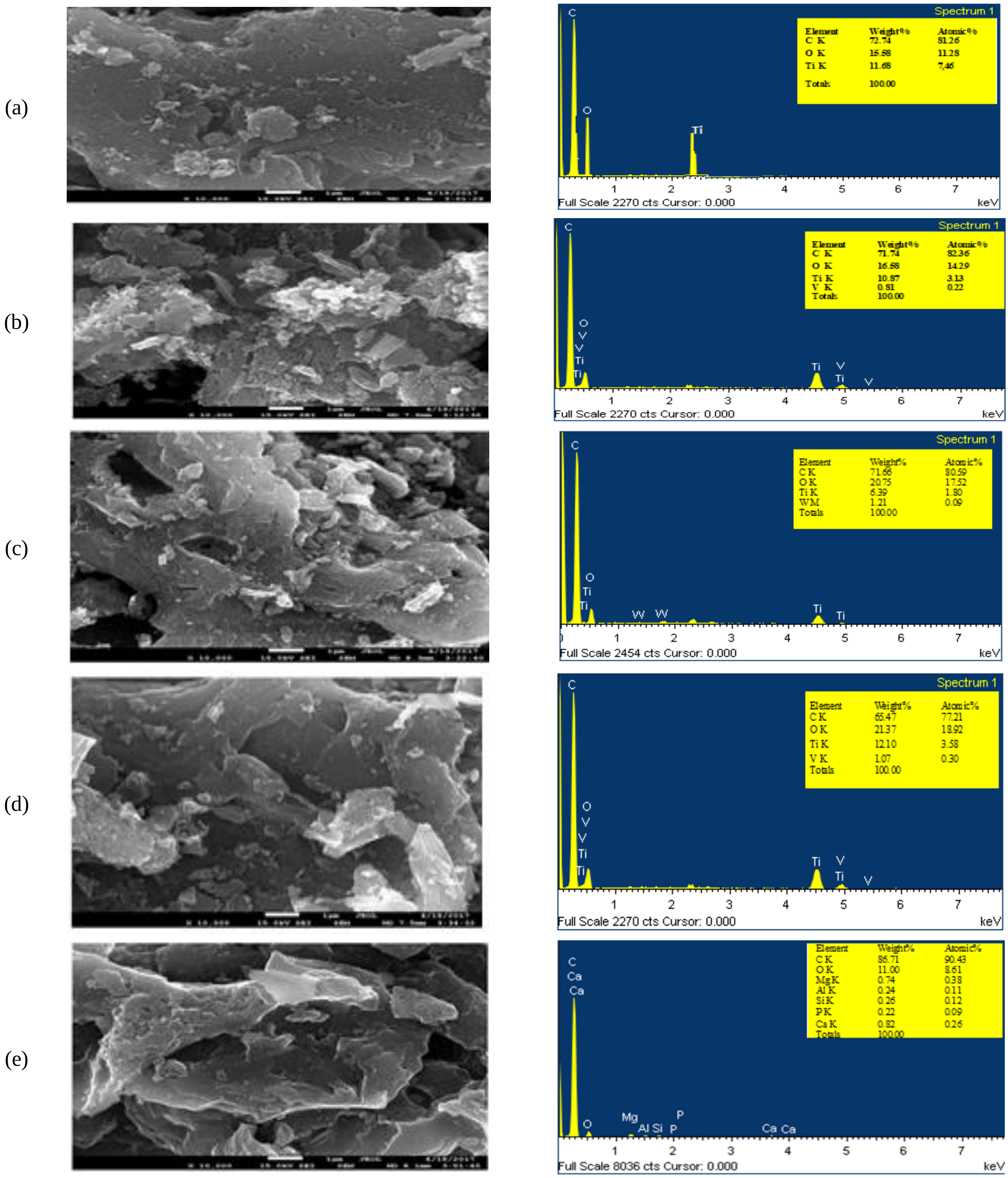

Fig. 2: SEM images of synthesized catalysts (a-TiO_2/AC, b-V_2O_5/TiO_2/AC, c-WO_3/TiO_2/AC, d-WO_3/V_2O_5/TiO_2/AC and e-AC).

When the literature studies are examined, the changes in the surface morphology of the prepared nanocomposite materials are better understood with SEM images and EDX analyses [31]. When the SEM images of all samples are examined from Fig. 2, it is seen that there is a homogeneous structure on the surface of the AC samples. On the other hand, when the catalytic materials are kept on this material, it is seen that the homogeneous structures are lost on the surface in general. Here. it is generally thought that the catalytic materials are adsorbed on the surface and form aggregates.

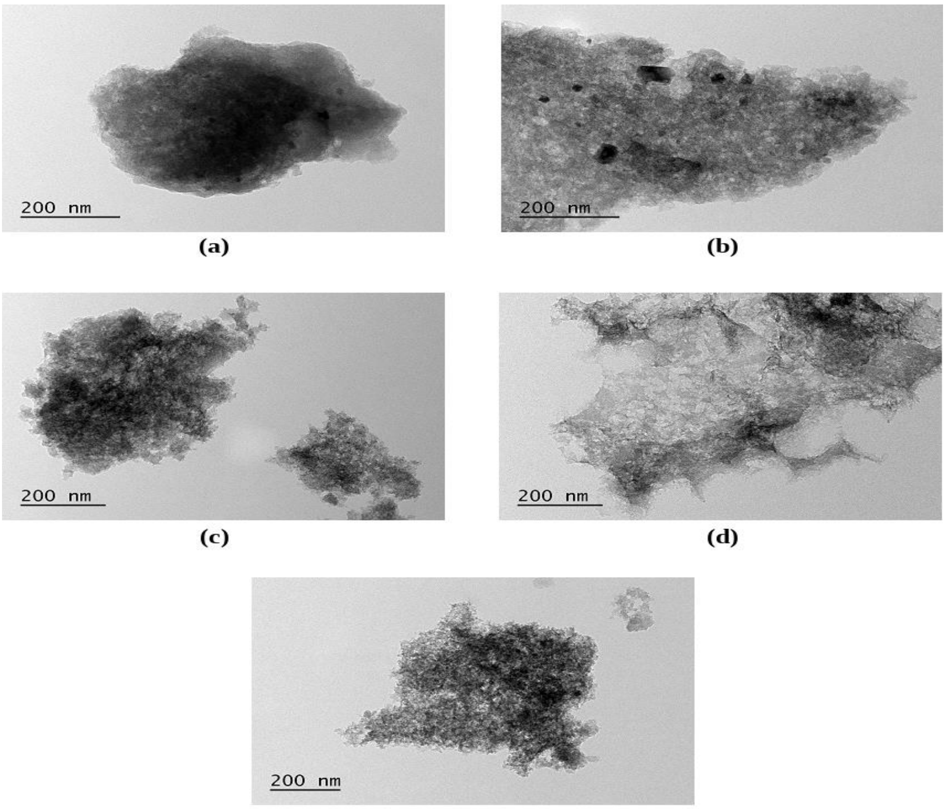

(a) (b)

(c) (d)

(e)

Fig. 3: TEM images of synthesized catalysts (a-TiO_2/AC, b-V_2O_5/TiO_2/AC, c-WO_3/TiO_2/AC, d-WO_3/V_2O_5/TiO_2/AC, e-AC).

Especially in the sample of V_2O_5/TiO_2/AC, this situation is observed more clearly. As shown in Fig. 2, the quantitative results of EDX give the percent weight elements of the synthesized composite materials. According to the results obtained, while there are certain elements in the activated carbon sample at the beginning, there is a variation in the percentage compositions according to the substances loaded on it later on. In similar studies, when the data obtained from EDX analyzes are evaluated, it is emphasized how the material has shape and composition [32,33]. As a result, the findings from the EDX analysis are in agreement with the XRD results. It is seen that the percentages of elements present in all catalytic samples vary significantly and the elements are significantly covered on the surface. This shows that nanoparticles with catalytic properties interact well with activated carbon.

TEM analysis

The TEM images of the used catalytic materials are shown in Fig. 3.

When the TEM images of all samples are examined from Fig. 3, it is seen that there is a clear structure on the surface of the AC samples. On the other hand, when other catalytic materials are examined, it is seen that the permeable surface on which homogeneous structures are distributed on the surface is more visible. When the TEM images of TiO_2/AC and WO_3/TiO_2/AC samples are examined, a distinctive homogeneity is observed here. In general, lace structure is observed more prominently in these examples. In addition, Fig. 3(a) shows the effects of catalytic gasification and abrasions in AC samples. In other samples, some larger mobile catalytic particle abrasions in certain sizes are observed at the edge of the catalytic materials and particles in general. It is thought that the channelling that occurs here may help the porosity size and the transport of the adsorbate to the interior of the particle.

FT-IR Analysis

The TiO_2/AC spectra showed stretching vibration at 3440 cm^{-1} associated with the stretching vibration of hydroxyl groups (–OH). This indicates the presence of hydroxyl functional groups on the surface of your TiO_2/AC material. C–H Stretching at 2923 cm^{-1} related to the stretching vibration of carbon-hydrogen bonds,

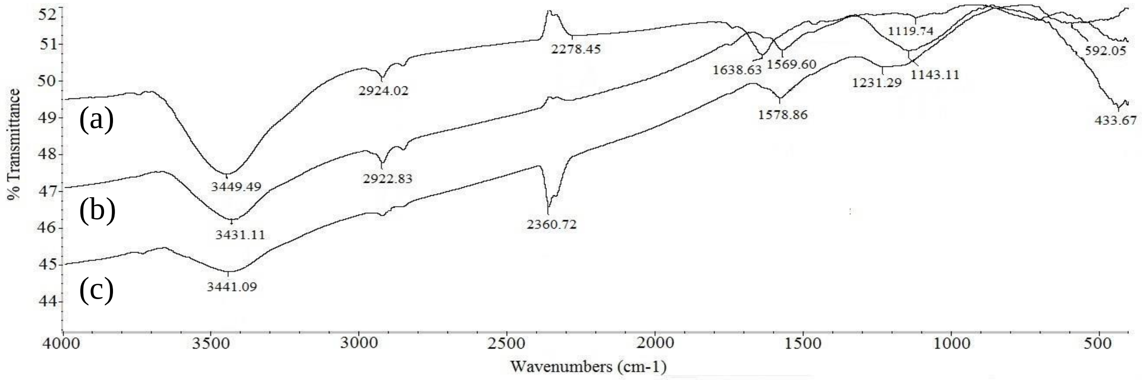

Fig. 4: FT-IR spectra belonging to TiO_2/AC (a), TiO_2/V_2O_5/AC (b) and TiO_2/WO_3/AC (c)

specifically $–CH_2$ groups indicating the presence of methylene groups on the surface. The band height and broadness of these peaks did not change after the application of TiO_2. This suggests that the presence of TiO_2 did not significantly alter the concentrations or properties of the hydroxyl and methylene groups on the activated carbon surface. The disappearance of band at 1575 cm^{-1} which is related to the stretching vibration of aromatic C=C bonds, indicates a change in the chemical composition of the material. The disappearance of this peak suggests that the aromatic C=C bonds may have been affected or replaced by a different chemical group. Also, the appearance of band at 1638 cm^{-1}attributed to titanium carboxylate, suggests the formation of a new chemical bond involving titanium and carboxylate groups presenting the interaction between TiO_2 and carboxyl functional groups on the activated carbon surface (Fig. 4a). Hydroxyl band on TiO_2/V_2O_5/AC Surface decreased in intensity, and it also underwent a shift to a lower wavenumber, specifically to 3431 cm^{-1}. This shift suggests a change in the hydrogen bonding environment or in the chemical nature of the hydroxyl groups.

Comparison with WO_3 it is noted that the $–CH_2$ bands on the TiO_2/V_2O_5/AC surface were unaffected, implying that these groups remained unchanged during the reaction. However, the hydroxyl groups (–OH) were involved in the reaction, leading to their decrease and spectral shift. The shifting of C=C Band to 1569 cm^{-1} after the reaction of the material with V_2O_5 suggests a change in the electronic environment or bonding nature of the aromatic C=C groups on the surface. Also, the shift of C–O band at 1156 cm^{-1} in pure AC to 1143 cm^{-1} after the removal of titanium carboxylate and the subsequent reaction with V2O5. This shift indicates a change in the oxygen-carbon bonding environment, possibly due to the removal of certain functional groups and the introduction of new species (Fig. 4b). The hydroxyl band shifted from 3440 cm^{-1} to 3441 cm^{-1} after the addition of WO_3. This shift suggests a subtle change in the hydrogen bonding environment or like the hydroxyl groups on the surface of the TiO_2/WO_3/AC material. Not only did the hydroxyl band shift, but the area under the peak also decreased. This reduction in area could indicate a change in the concentration or environment of hydroxyl groups on the surface. In addition, the disappearance of the $–CH_2$ band at 2924 cm^{-1} after the addition of WO_3 indicates that the methylene groups ($–CH_2$) may have been affected or altered during the reaction with WO_3 (Fig. 4c). The observed shifts in the hydroxyl (–OH) band, the disappearance of the $–CH_2$ band, and the decrease in the area under the –OH peak after the addition of WO_3 provide strong evidence that WO_3 has indeed affected these functional groups on the TiO_2/WO_3/AC material. These changes suggest chemical interactions between WO_3 and the surface functional groups, leading to modifications in their vibrational properties. The disappearance of the band related to titanium carboxylate, the appearance of a new peak at 1578 cm^{-1}, and the emergence of a band at 1231 cm^{-1} related to W=O provide compelling evidence for the addition of WO_3 to the material. These changes in the spectral features point to the introduction of tungsten oxide (WO_3) species on the surface, which is consistent with the expected reaction or impregnation process.

XRD analysis

Fig. 5(a) shows the XRD spectrum of activated carbon. The peak with the highest intensity at $2\theta = 26.67$ belongs to the hexagonal graphite phase (JCPDS card number 75–1621).

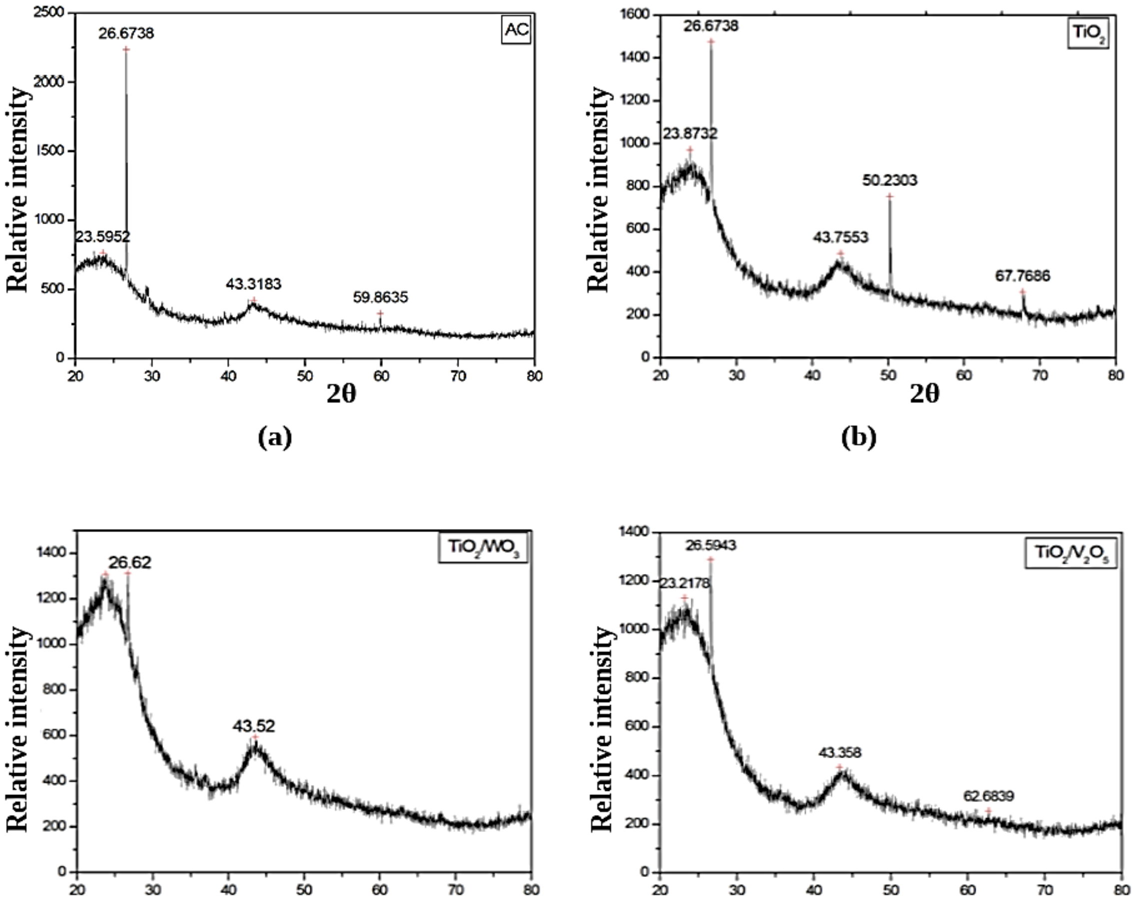

(a) (b)

(c) (d)

Fig. 5: XRD spectrums of the catalysts.

This also shows the high crystalline nature of graphite. Other peaks were evaluated as 2θ =23.59°, 43.31° and 59.86° characteristic lower amorphous peaks of Activated Carbon [34].

Fig. 5(a) shows the XRD spectrum of activated carbon. The peak with the highest intensity at 2θ = 26.67 belongs to the hexagonal graphite phase (JCPDS card number 75–1621). This also shows the high crystalline nature of graphite. Other peaks were evaluated as 2θ =23.59°, 43.31° and 59.86° characteristic lower amorphous peaks of Activated Carbon [34].

Fig. 5(b) shows the XRD spectrum of TiO_2/AC. As known, TiO_2 can be found in 3 different forms such as anatase, rutile and brookite phases [35]. 2θ degrees at 23.8732°, 26.67°, 43.7553°, 50.2303° and 67.7686° values seen above define the rutile form of TiO_2 (JCPDS 75-1537). Sharp and severe peaks indicate that TiO_2/AC has high crystallinity.

Fig. 5(c) shows the XRD pattern of WO_3/TiO_2/AC. The main peaks of both monoclinic WO_3 and anatase TiO_2 are very close to each other indicating the effective immobilization of WO_3 onto the TiO_2/AC surface [30]. These results were also supported by the shifting of the 2 theta degree to the left (from 26.67 to 26.62) and decreasing the peak intensity resulting in effective stress (Uniform strain) of WO_3 within the TiO_2 lattice structure [36].

The XRD spectrum of the V_2O_5/TiO_2/AC composite material is shown in Fig.5(d). The 2θ value at 23.2178 in this pattern indicates the ortho-rhombic crystal structure of V_2O_5 (JCPDS 89-0612). Also, it is concluded that the slight decrease in peak intensity of TiO_2 presents effective anchored of V2O5 in V_2O_5/TiO_2/AC sample [37].

BET and Pore Analysis

In the present study, BET analyses, pore size and pore volumes were analyzed by taking commercial AC. The results of the BET test are presented in Fig. 6. AC, TiO_2/AC, WO_3/TiO_2/AC, V_2O_5/TiO_2/AC and WO_3/V_2O_5/TiO_2/AC BET

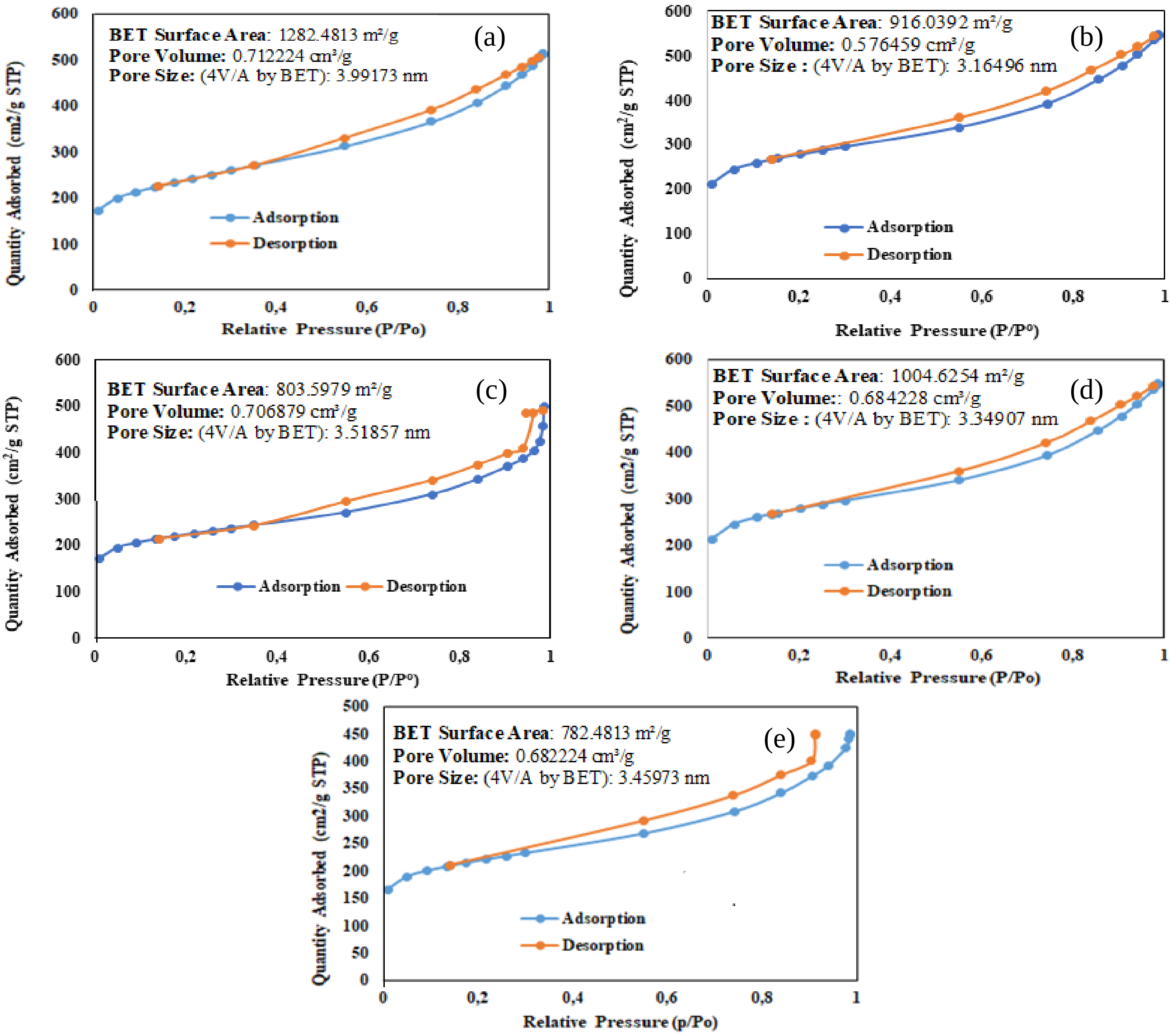

Fig. 6: BET analyses, pore size and pore volumes (a-AC, b-TiO_2/AC, c-WO_3/TiO_2/AC, d-V_2O_5/TiO_2/AC, e-WO_3/V_2O_5/TiO_2/AC).

surface areas are respectively 1282.48 m^2/g, 916,039 m^2/g, 803.59 m^2/g, 1004.62 m^2/g and 782,481 m^2/g. Modifying the catalytic materials with AC showed a partial reduction in BET surface areas and pore volumes compared to the raw sample. This is thought to be due to the adsorbing of materials to the AC surface and partially filling its pores. This may be associated with the formation of porosity and roughness [38]. There is quite a lot of organic matter in OMW These molecules generally contain tannin, lignin, fatty acids and polyphenolic compounds. Therefore, it is not easy to compare the pore sizes and diameters of the existing samples with the components of black water. Based on the International Union of Pure and Applied Chemistry (IUPAC) classification, it is reported that if the diameters of the particles are less than 2 nm, between 2–50 nm and greater than 50 nm, they belong to the microporous, mesoporous and macroporous groups, respectively [30]. In general, it is seen that the pore diameters are in the range of 3 to 4 nm for all samples. This means that the adsorption process mainly takes place in physical form, and it is thought that adsorbents modified with oxides may have high adsorption capacity and electrocatalytic effect [29]. Also, the N_2 adsorption-desorption is approximately equal for all studied materials. The IUPAC classification is reported to belong to type IV, whose N_2 adsorption-desorption isotherm corresponds to the mesoporous nature of adsorbents [39].

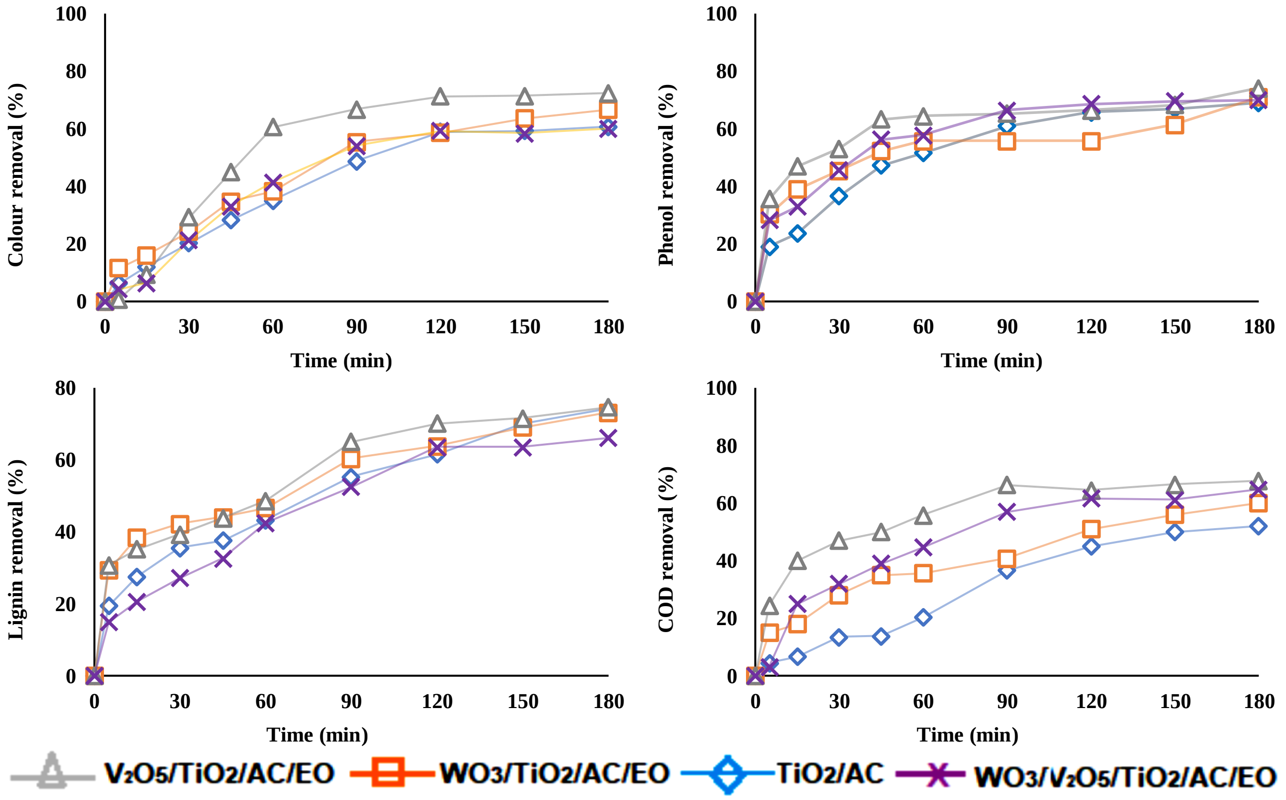

***Fig. 7:** Removal rates over time with particle electrodes of different properties (20Volt, 1.0 g/L^{1} NaCl, 1.0 g/L catalyst and pH≈5,5)*

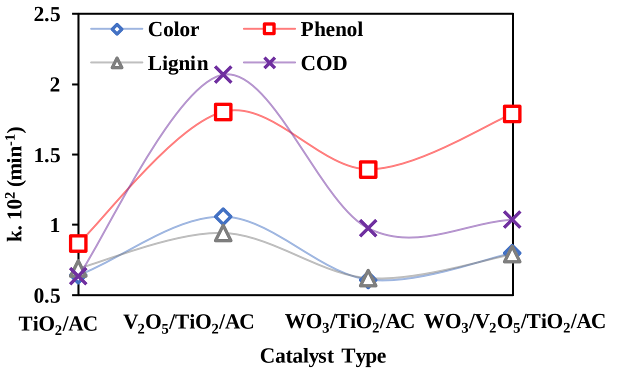

***Fig. 8:** Continuous or pace curves for each category of catalyst (These curves show the reaction rate constant (k) values with particle electrodes of different properties (20Volt, 1.0 g/L NaCl, 1.0 g/L catalyst and pH≈5,5).*

Electrocatalytic Oxidation

The electrocatalytic use of nanocomposite materials prepared in 4 different compositions in the form of particle electrodes in olive-black water was investigated. Since the conductivity of the black water was not sufficient, 1 g/L NaCl was added as a supporting electrolyte. In all experimental studies, the degradation efficiency of the olive black water was monitored by investigating the changes in the concentration of colour, phenol, lignin and COD over time. The catalyst sample with the highest removal rate was used as a working electrode and the removal rates obtained in different parameters were discussed under the headings.

Catalyst Effect

Three-phase electrochemical processes generally consist of a material called particulate electrode or bed electrode and filled granular or crushed materials between two counter electrodes. Here, a suitable voltage can polarize the particles to form a large number of charged microelectrodes and form oppositely charged structures, one of which can be considered an anode and the other a cathode [21]. This shows that with the presence of particle electrodes, the three-phase electrochemical process outperforms the other conventional two-phase electrochemical systems. In the presented study, with experiments using TiO_2/AC, WO_3/TiO_2/AC, V_2O_5/TiO_2/AC, and WO_3/V_2O_5/TiO_2/AC catalysts; Color, phenol, lignin, and COD removal rates were measured depending on time. The results obtained are given in Figs. 7 and 8. By examining these results, the removal rates were investigated depending on the voltage, catalyst amount and initial pH value with the particle electrode showing the highest performance.

When the colour removals according to the catalyst type were examined, it was observed that the $V_2O_5/TiO_2/AC$ catalyst showed the highest removal rate with a removal rate of 72 % at the end of 3 h, while the second highest removal rate was observed for $WO_3/TiO_2/AC$ with 66 %. For $V_2O_5/TiO_2/AC$, this value was reached within 1.5 h. When the phenol removal rates were examined, the removal rates of 4 different catalysts after 3 h ranged between 69 % and 74 % and the highest phenol removal was observed for $V_2O_5/TiO_2/AC$. When the lignin and COD removal rates were examined, the highest rates were observed for $V_2O_5/TiO_2/AC$ at 74.6 % and 67.7 %. respectively. This shows that in general, the highest performance is achieved with the $V_2O_5/TiO_2/AC$ particle electrode. This led to subsequent experiments being conducted with these particle electrodes. In the literature studies, it is reported that both electrochromic and photocatalytic properties of vanadium pentoxide (V_2O_5) are evident. In addition, it is stated that vanadium doping affects both the optical band gap (forming close to the valence or conductive bands) and the electron-hole recombination kinetics [40]. İt can be explained by its greater catalytic effect.

The reaction mechanism is quite complex to explain, as the mechanism for removing contaminants in the three-phase electrochemical process is dependent on the nature of wastewater pollutants, electrode materials as well as the type of particulate electrode used [42-44]. Also, except for the role of the particle electrode, the contributions of the electrochemical reactions in the electrodes are the same as in the other two-phase system. Located between both anode and cathode without direct electrical contact, these particles act as adsorbents and are thought to increase ionic charge distribution. In addition, oxidation reactions occur on both main electrode surfaces. Activated carbon was used as a support material in the present study due to its high surface area. Due to the large specific surface area and high porosity, the adsorption of pollutants to the particle electrode is inevitable. When an external electrostatic field is applied to the particle electrode surface immersed in an aqueous electrolyte solution, the two faces of the particles collect positive charges and negative charges. respectively. These charged ions have to shift to the opposite side of the charged particle electrodes and electrosorption occurs [21, 41-45]. The removal rates provided above with all microparticles suggest that the combination of adsorption and electrosorption plays an effective role and contributes significantly to the removal of organic pollutants.

Voltage Effect

The current density/cell voltage is one of the most important variable parameters of the three-phase system, as it affects not only the electrochemical oxidation but also the polarization behaviour of the particle electrodes [41]. With a suitable voltage/current density, the particles polarize to form microelectrodes that can enhance electrosorption or oxidation. In the present experimental study, the voltage effect was carried out with the $V_2O_5/TiO_2/AC$ catalyst, which showed the highest removal performance when the catalyst effect was evaluated and the removal rates were compared for 10, 20 and 30 Volts according to previous studies [46]. The results obtained are presented in Figs 9 and 10.

The results obtained show that the colour removal rate can reach up to 35 % after 3 h of testing when a 10 V voltage is applied to the electrodes. This value increased to 72 % after 3 h for 20 V, for 30 V the value increased to 80 % after 3 h. While 53% removal of phenol was achieved for 10 V, this value increased to 74 % and 85 % for 20 and 30 Volts, respectively. For lignin, the percentage removal was 51 %, 68 % and 74 % respectively. In addition, when the removal percentages are taken into account, a linear performance increase is observed with the voltage increase but there is a lower trend between 20 V and 30 V. When the reaction kinetics are evaluated, although a significant difference is observed for 30 V, it is seen that 20 V may be sufficient when the total energy consumed is taken into account. In similar studies, it is reported that when current density or cell voltage is used, the performance increases with the increase in energy consumption [47-48]. In many studies, it is reported that the main driving force of electrochemical degradation is voltage and the observed increase in this parameter significantly increases the COD and colour removal efficiency of many wastewaters [49]. For this reason, it is thought that optimum experimental design may be important in terms of energy consumption in removal efficiency and energy consumption.

Solid/Liquid Ratio Effect

The three-phase electrode (TPE) system is a method that can support the study of both reactions, including ion

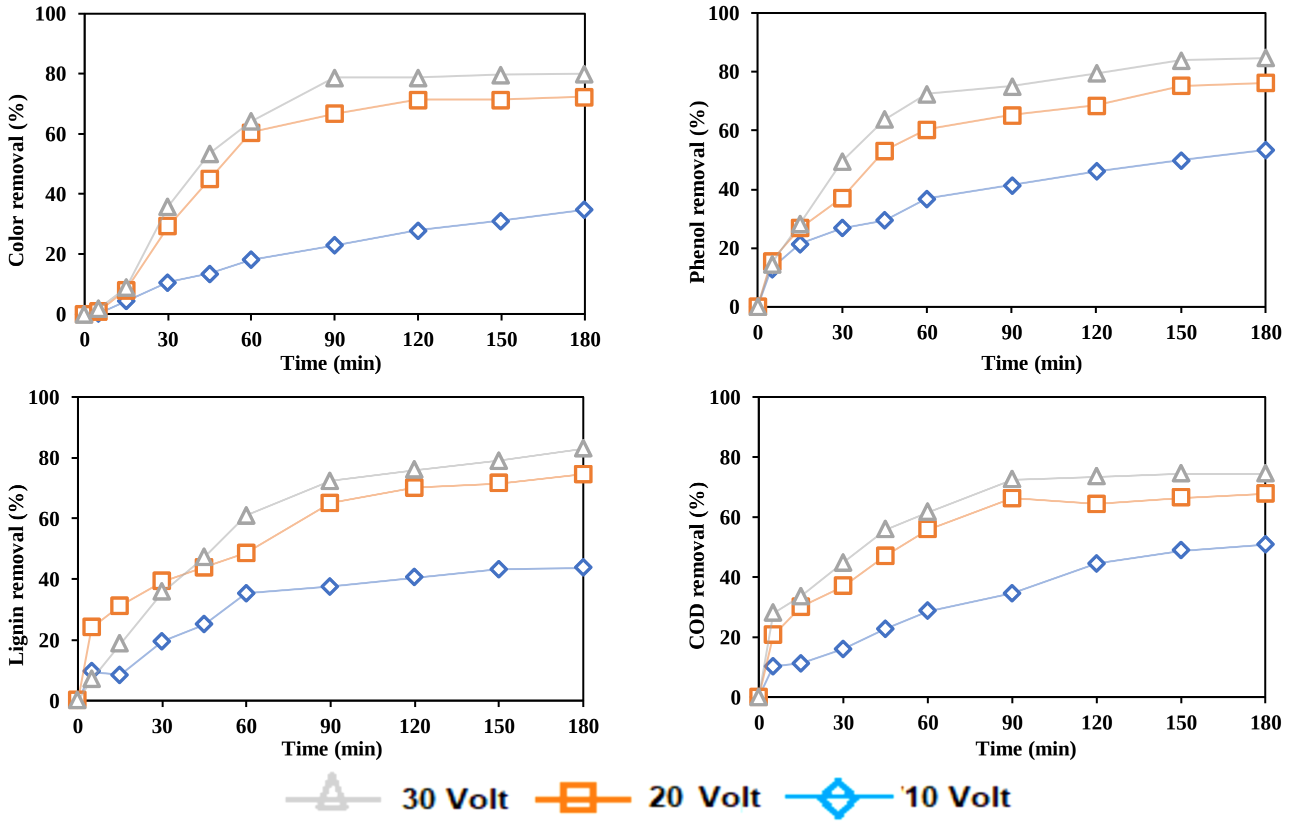

Fig. 9: Removal rates over time depending on voltage (1.0 g/L NaCl, 1.0 g/L $V_2O_5/TiO_2/AC$ and pH≈5,5)

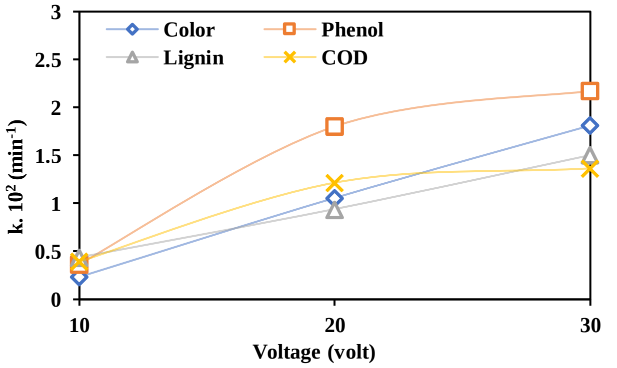

Fig. 10: Changes in reaction rate constant (k) values according to the electrical voltage applied to the particle electrodes (1.0 g/L NaCl, 1.0 g/L $V_2O_5/TiO_2/AC$ and pH≈5,5)

and electron transfer. Here, besides two electrodes, there is also a working electrode [50]. These processes are applied in the treatment of many organic and inorganic wastewater as well as in the regeneration of adsorbents. However, small changes in variables such as electrode position, aeration and electrolyte concentration make a difference in the overall removal rate. In addition, the particle electrode may cause reductions in its adsorption capacity and catalytic activity due to the accumulation of contaminants on the surface during continuous operation. In the present study, color, phenol, lignin, and COD removal rates were investigated by using electrodes with 0.5 g/L, 1.0 g/L and 1.5 g/L ratios to examine the effect of solid/liquid ratio on removal using $V_2O_5/TiO_2/AC$ catalyst. The results obtained are given in Figs. 11 and 12.

When the effect of the changes in the solid/liquid ratios on the yield was examined, generally less yield was obtained at 0.5 g/L ratios. It is observed that the chromaticity is approximately 80 % at the end of 3 h with 1.0 g/L and 1.5 g/L, 80 % for phenol and lignin and 70 % for COD removals. Partial removal at high solid/liquid ratios is associated with higher adsorbing effects of particle electrodes and, accordingly, more intense interaction of the catalytic effect.

In three-phase systems, apart from the main electrodes in the electrochemical cell, the particle electrode material plays a very important role. Good particle electrode materials, good adsorption capacity, high electrocatalytic activity, good conductivity and large specific areas can be listed as properties that will increase the removal efficiency.

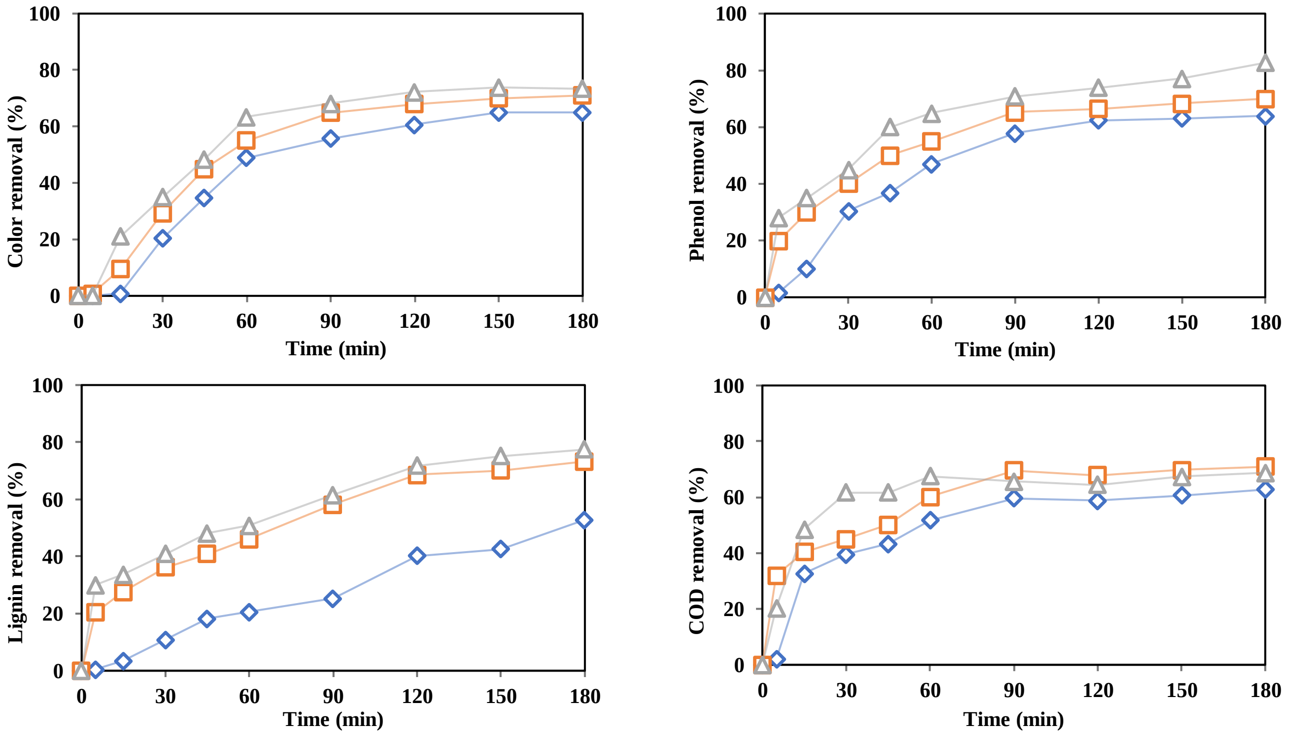

Fig. 11: Removal rates over time depending on solid/liquid ratio (20Volt, 1.0 g/L NaCl, $V_2O_5/TiO_2/AC$ and pH ≈ 5,5)

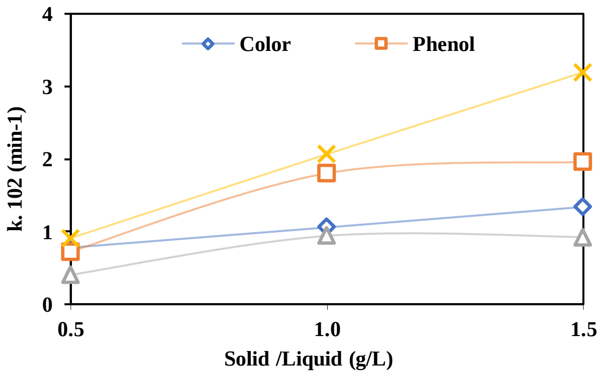

Fig. 12: Changes in reaction rate constant (k) values according to solid/liquid ratio ($V_2O_5/TiO_2/AC$, 20Volt, 1.0 g/L NaCl and pH ≈ 5,5).

In addition, promoters are needed to increase the heterogeneous properties of the particle electrode and the increase in the amount of catalyst is an important factor. It is thought that it contributes significantly to the electrocatalytic performance with the increase in the type and ratio of the catalyst coated on the particles.

pH Effect

Initial pH is a very important parameter in three-dimensional electrocatalytic systems because conditions such as direct oxidation, indirect oxidation and AC regeneration can significantly affect the yield [51-53]. In addition, the pH of the suspension can affect the adsorbing performance and properties of the particle electrode [40]. In studies using 1.0 g/L $V_2O_5/TiO_2/AC$ catalyst, color, Phenol, lignin and COD removal rates were examined according to the initial pH value. The results obtained are presented in Figs. 13 and 14.

When the data in Figures 13 and 14 are examined, it was observed that COD removal was high at both low and in the pH range of 5 to 6, while the color removal rates were fixed at all pH values after 3 h (70 %). On the other hand, it was observed that 70 % of phenol and lignin were removed at the end of 3 h at all values except pH: 7.0 and 9.0 in the pH range of 5 to 6. In similar studies, it has been reported that an increase in pH value causes adverse effects on anodic oxidation and indirect oxidation as well as color and COD removal. This shows that the efficiency may decrease as oxygen formation due to side reactions that may occur on the surface of the electrodes at high pH increases anodic oxidation. It is reported that this can only be overcome if H_2O_2 is produced electrochemically in a more alkaline solution [41].

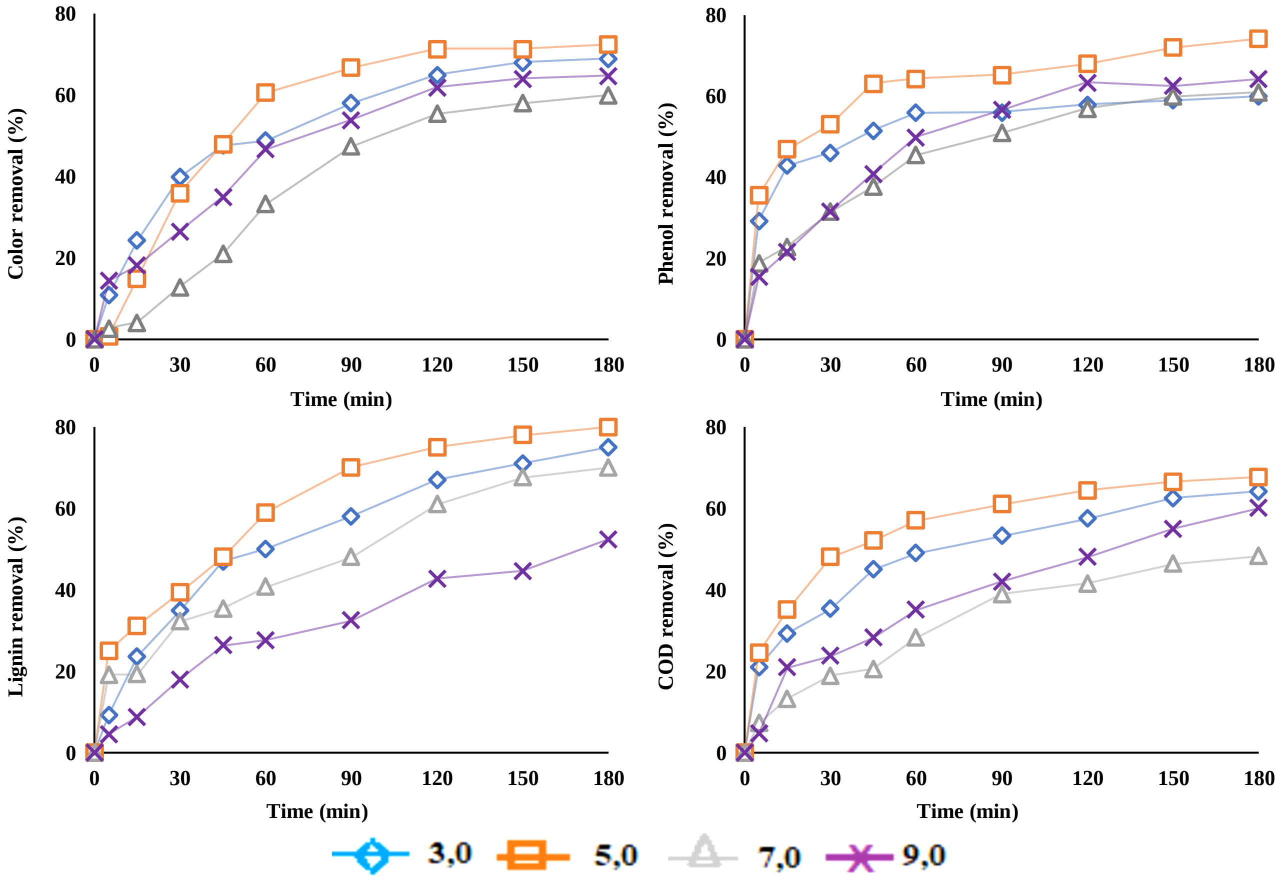

Fig. 13: Removal rates over time depending on the initial pH value (20 Volt, 1.0 g/L NaCl, 1.0 g/L $V_2O_5/TiO_2/AC$)

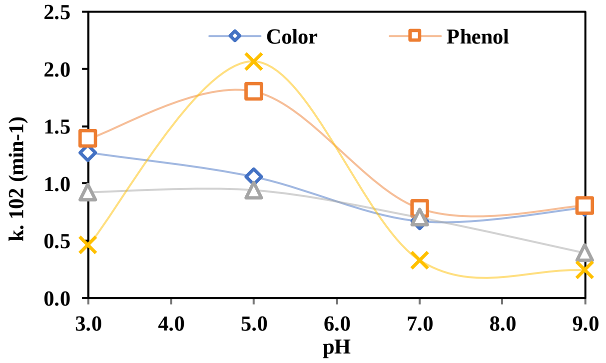

Fig. 14: Changes in reaction rate constant (k) values according to initial pH value (20Volt, 1.0 g/L NaCl, 1.0 g/L $V_2O_5/TiO_2/AC$ and pH≈5,5)

Adsorption, Electrooxidation and Electrocatalytic Oxidation Effect

It is reported that the degradation mechanisms of organic substances in three-phase systems are complex and there may be two different pathways in general, (1) Direct oxidation of organic molecules by direct electron transfer reaction; (2) indirect oxidation by hydroxyl radicals and aqueous oxidants such as hydrogen peroxide [54]. It has been reported in similar studies that the decomposition of organic substances can form ring-opening products such as carboxylic acids and the final product of CO_2 and the formation of some aromatic intermediates that are finally can be oxidized, and that the colouring chromophore groups, especially in dyes, can be destroyed [55-56]. In the present study, for better elucidation of the electrocatalytic oxidation effect; experiments with particle electrode adsorption, electrooxidation (two-phase), and electrocatalytic oxidation (three-phase) were carried out separately. The results obtained are presented in Figs. 15 and 16.

When Fig. 16 is examined, it is seen that the removal efficiency is very low in all species when only particles are used and adsorbed (without electrochemical oxidation). It is observed that the efficiency is slightly increased when only electrooxidation experiments are carried out without working

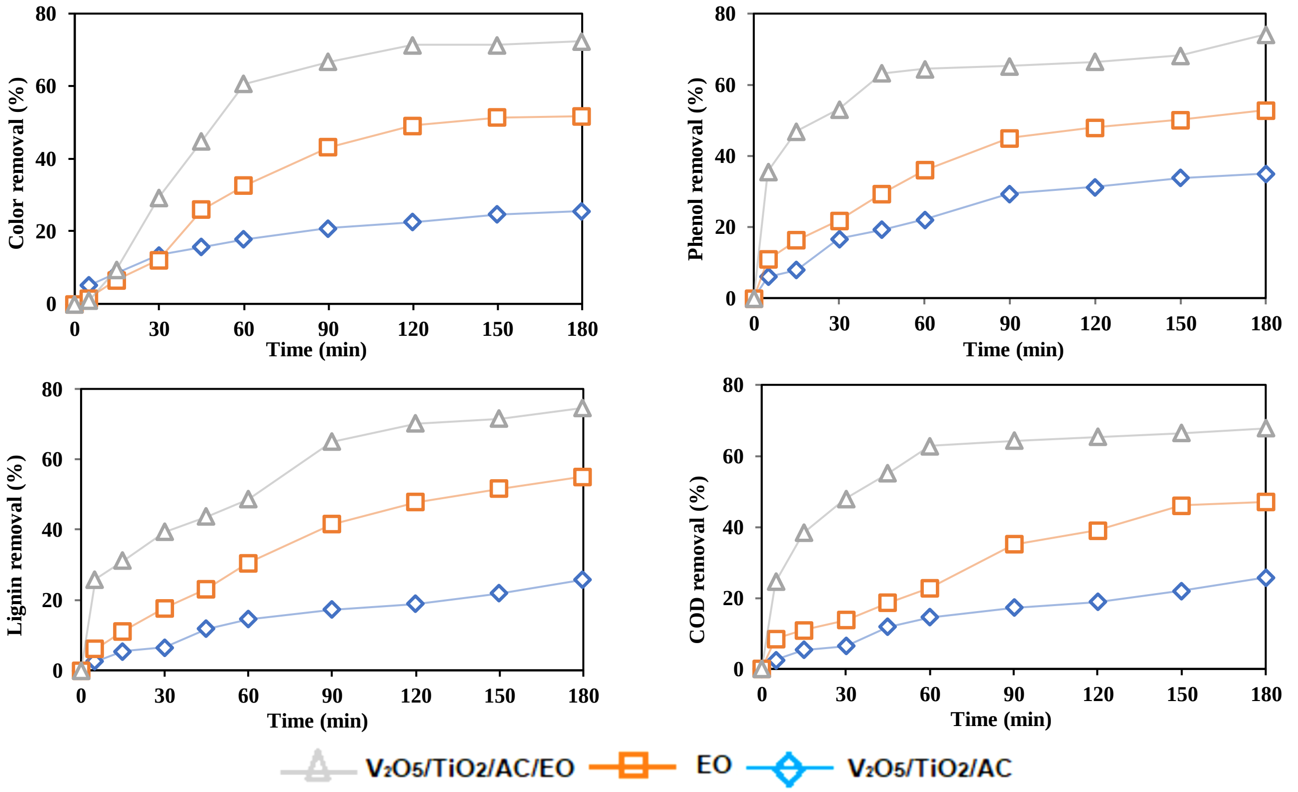

Fig. 15: Adsorption effect; electrooxidation effect and electrocatalytic oxidation effect (20 Volt, 1.0 g/L NaCl, 1.0 g/L and $V_2O_5/TiO_2/AC$)

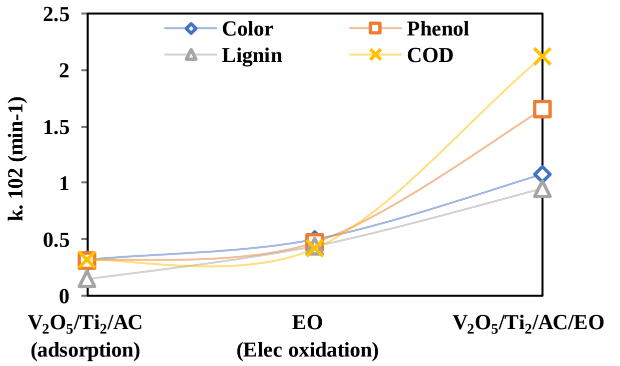

Fig. 16: Adsorption effect; Changes in reaction rate constant (k) values for electrooxidation effect and electrocatalytic oxidation effect ($V_2O_5/TiO_2/AC$, 20Volt, 1.0 g/L NaCl, and pH≈5,5).

electrodes. this shows that it is due to surface interaction only. It shows that the efficiency can be much higher when the working electrode and carbon electrode are used together. This result can be associated with the distribution of the electrons throughout the liquid, the expansion of the electrode surface areas and the higher diffusion rate. In other words, it has been observed that the 3-phase system is more successful than the two-phase system.

Proposed Electrocatalytic Mechanism

Although three-phase systems are more efficient, however, their degradation mechanism may be more complex. We believe that the type of wastewater, electrode materials and particle electrode will play an important role in the removal of pollutants from OMW. In the present study, the schematic of the electrocatalytic assembly was designed by taking into account similar studies done previously and is shown in Fig. 17. It is thought that the role of the electrode, which is synthesized as a nanoparticle and expressed as a particle electrode, can exhibit behaviour such as adsorbing the particles located between both the anode and the cathode and increasing the ionic charge distribution without direct electrical contact. In addition, it is suggested in similar studies that possible main reactions (direct oxidation or indirect oxidation) may occur on the electrode surface in this system [54-57].

In classical electrooxidation systems, the mechanism for the anodic oxidation of pollutants in aqueous solutions is generally divided into two categories: 1) direct oxidation (direct electron transfer on the anode) and 2) indirect oxidation (electrochemical oxidizing species. e.g.,

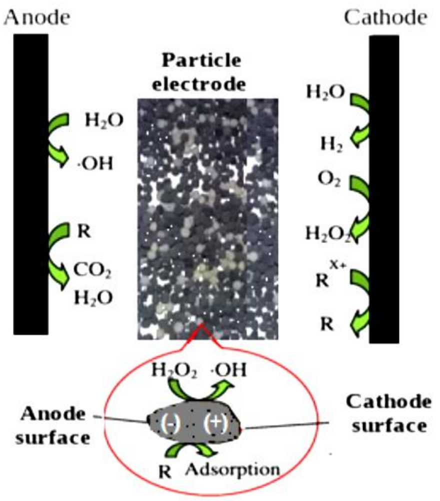

Fig. 17: Suggested scheme of electrocatalytic removal using a combination of nanoparticle electrode and graphite electrode

hydroxyl radicals) [52]. It is reported that in indirect oxidation, adsorbed hydroxyl radicals can be produced from the electrolysis of wastewater and interact with organic substances and adsorbed hydroxyl radicals can interact with organic compounds by different mechanisms [53].

$$\text{Orgc matter} + H_2O \rightarrow \text{Orgc matter}\ ^{\cdot}OH) + H^+ + e^- \qquad (2)$$

$$\text{Orgc matter}\ (^{\cdot}OH) \rightarrow \text{Orgc matter (O)} + H^+ + e^- \qquad (3)$$

$$\text{Orgc matter}\ (O^*) \rightarrow \text{Iintermediate Orgc compound} + CO_2 + H_2O \qquad (4)$$

Similar studies show that particle electrodes not only act as an adsorbent but also act as a catalyst for the generation of hydroxyl radicals that increase oxidation [44]. It is known that olive black water contains a significant number of phenolic compounds. It is reported that hydroxyl radicals formed on the surface of the catalyst and electrodes easily attack the aromatic ring in the phenolic structure. Firstly, to form dihydric phenol or quinone and then ring-structured carbonyl compounds and carboxylic acids and finally H_2O and CO_2 are formed [46-47].

Kinetic Data

The degradation kinetics of the catalysts used were obtained by linearizing the Preudo (pseudo) 1st order velocity equation specified in (5).

$$\text{Ln}\ (C_t/C_o) = -kt \qquad (5)$$

Here, C_o is the initial concentration of wastewater (mg/L), C_t is the concentration at time t (mg/L), t is time and k is the pseudo 1st order rate constant, which has been proven by regression analysis ($R^2 > 0.70$). The higher rate constant obtained by using the catalyst can be explained by the combined effects of the adsorption of the organic molecule on the catalyst surface and the oxidation that occurs with the direct attack of the hydroxyl radicals produced on the positive spaces formed afterwards [42,58]. The reaction rate constants of electrocatalytic oxidation processes are given in Table 3 respectively.

When Table 3 is examined, it is seen that the data obtained in all separations provide first-degree conformity of over 90 %. In addition, when the degradation states per unit time are examined, it supports the view that especially low molecular weight materials decompose and oxidize faster, whereas biopolymeric materials such as lignin can degrade in a more difficult and high voltage environment. In addition, according to the results obtained in acidic conditions, it can be seen that its performance may be higher due to acid catalysis.

CONCLUSIONS

In this study, experimental studies on the treatment of OMW with electrocatalytic systems at different experimental parameters were carried out. For this purpose, TiO_2/AC, $V_2O_5/TiO_2/AC$, $WO_3/TiO_2/AC$, and $V_2O_5/WO_3/TiO_2/AC$ catalysts were synthesized. In studies on the structural characterization of catalysts, it has been observed that semiconductor materials with catalytic effects adhere well to the activated carbon surface. When the results obtained as a result of the use of catalytic in different parameters are briefly evaluated, with the electrocatalytic oxidation method color and COD removal were obtained without the need for any additional chemicals except NaCl, which is used as a supporting electrolyte. Significant color, lignin and COD removals were observed and the voltage effect contributed significantly to the electrocatalytic oxidation. However, the effect of the solid/liquid ratio on the removal was limited. Although the effect of initial pH values on electrocatalytic oxidation remained limited higher removal rates were generally achieved faster in an acidic medium.

As a result, it has been seen that the fastest and most effective method in the catalytic processes used for the treatment of olive black water is electrocatalytic oxidation. When the results of the study are evaluated, it is thought to have a commercial value. This study is preliminary research, and it has been concluded that the further

***Table 3: Reaction rate constant (k) and R^2 values of electrocatalytic oxidation*.**

Parameters	Color		Phenol		Lignin		COD	
	kx10^2(min^{-1})	R^2	kx10^2(min^{-1})	R^2	kx10^2(min^{-1})	R^2	kx10^2(min^{-1})	R^2
Catalyst type								
TiO_2/AC	0.641	0.97	0.869	0.94	0.691	0.98	0.637	0.95
V_2O_5/TiO_2/AC	1.058	0.98	1.804	0.92	0.942	0.96	2.067	0.89
WO_3/TiO_2/AC	0.611	0.96	1.395	0.93	0.621	0.91	0.976	0.99
WO_3/V_2O_5/TiO_2/AC	0.801	0.98	1.791	0.97	0.791	0.99	1.037	0.97
Voltage								
10V	0.234	0.98	0.369	0.91	0.439	0.97	0.394	0.97
20V	1.058	0.98	1.804	0.92	0.942	0.96	1.217	0.90
30V	1.813	0.99	2.173	1.00	1.504	0.99	1.366	0.97
Solid/liquid ratio								
0.5 g/L	0.780	0.98	0.727	0.97	0.405	0.98	0.911	0.91
1.0 g/L	1.058	0.98	1.804	0.92	0.942	0.96	2.067	0.90
1.5 g/L	1.340	0.96	1.959	0.97	0.925	0.95	3.195	0.95
pH								
pH = 3	1.271	0.96	1.390	0.93	0.924	0.94	0.460	0.97
pH = 5	1.058	0.98	1.804	0.92	0.942	0.96	2.067	0.90
pH = 7	0.670	0.98	0.782	0.97	0.702	0.99	0.330	0.96
pH = 9	0.790	0.98	0.807	0.96	0.392	0.97	0.242	0.97
Effect of each variable								
V_2O_5/Ti_2/AC (ads)	0.32	0.93	0.314	0.98	0.147	0.93	0.322	0.91
EO (Elec-oxidation)	0.5	0.92	0.473	0.96	0.442	0.92	0.424	0.90
V_2O_5/Ti_2/AC/EO	1.077	0.97	1.651	0.95	0.953	0.97	2.126	0.95

production of the material and its usability on an industrial scale can be an important reference for our future studies.

Acknowledgments

This work was supported by the Project Coordination Unit of Muğla Sıtkı Koçman University within the scope of project number 16/146.

Received: May 14, 2023; Accepted: Aug. 07, 2023

REFERENCES

[1] Elayeb R., Njehi M., Majdoub H., Trigui1M., Achour S., Optimization of the Electrocoagulation Process by Central Composite Design for Olive Mill Wastewater Decolorization and Removal of Polyphenols, *Inter. Res. J. Advanced Eng. Sci.*, **6(2):** 182-200 (2021).

[2] Foroutan R., Peighambardoust S.J., Mohammadi R., Peighambardoust S.H., Ramavandi B., Cadmium Ion Removal from Aqueous Media Using Banana Peel Biochar/Fe_3O_4/ZIF-67, *Environmental Research Volume*, **211:** 113020 (2022).

[3] Foroutan R., Mohammadi R., Ramavandi B., Bastanian M., Removal Characteristics of Chromium by Activated Carbon/$CoFe_2O_4$ Magnetic Composite and Phoenix Dactylifera Stone Carbon, *Korean J. Chem. Eng.*, **35(11):** 2207-2219 (2018).

[4] Peighambardoust S.J., Foroutan R., Peighambardoust S.H., Khatooni H., Ramavandi B., Decoration of Citrus Limon Wood Carbon with Fe_3O_4 to Enhanced Cd^{2+} Removal: A Reclaimable and Magnetic Nanocomposite, *Chemosphere*, **282:** 131088 (2021).

[5] Al Malah K., Azzam M.O.J., Abu Lail N.I., Olive Mill Effluent (Ome) Wastewater Post-Treatment Using Activated Clay, *Separation and Purification Technology*, **20:** 225-234 (2000).

[6] Aktaş E., Imre S., Ersoy L., Characterization and Lime Treatment of Olive Oil Mill Wastewater, *Water Research*, **35(9):** 2336-2340 (2001).

[7] Meyssami B., Kasaeian A.B., Use of Coagulants in Treatment of Olive Oil Wastewater Model Solutions by Induced Air Flotation, *Bioresource Technology* **96(3):** 303-307 (2005).

[8] Kiril B.M., Kestioğlu K., Yalılı Kılıç M., Zeytinyağı Endüstrisi Atıksularının Kimyasal Arıtma Sonrası Evsel Atıksularla Birlikte Arıtılabilirliğinin Respirometrik Yöntemle Araştırılması, *Ekoloji*, **17(66):** 39-46 (2008).

[9] Ginos A., Manios T., Mantzavinos D., Treatment of Olive Mill Effluents By Coagulation–Flocculation–Hydrogen Peroxide Oxidation and Effect on Phytotoxicity, *Journal of Hazardous Materials*, **133(1-3):** 135-142 (2006).

[10] Chedeville O., Debace M., Porte C., Removal of Phenolic Compounds Present in Olive Mill Wastewaters by Ozonation, *Desalination*, **249:** 865-869 (2009).

[11] Uğurlu M., Yılmaz S İ. Vaizoğullar A.L., Removal of Color and Cod From Olive Wastewater by Using Three-Phase Three-Dimensional (3D) Electrode Reactor, *Materials Today: Proceedings*, **18(5):** 1986-1995 (2019).

[12] Tezcan Ün Ü., Altay Ü., Koparal A.S., Bakir Öğütveren Ü., Complete Treatment of Olive Mill Wastewaters by Electrooxidation, *Chemical Engineering Journal*, **139:** 445-452 (2008).

[13] Rania E., Mondher N., Hatem M., Maher T., Sami A., Optimization of the Electrocoagulation Process by Central Composite Design for Olive Mill Wastewater Decolorization and Removal of Polyphenols, *International Research Journal of Advanced Engineering and Science*, **6(2):** 182-200 (2021).

[14] Uğurlu M., Kula İ., Gürses A., Removal of Some Organic Compounds and Color from Olive Mill Wastewater by Electrocoagulation, *Fresenius Environmental Bulletin*, **15(10):** 1256-1265 (2006).

[15] Gernjak W., Maldonado M.I., Malato S., Caceres J., Krutzler T., Glaser A., Bauer R., Pilot-Plant Treatment of Olive Mill Wastewater (OMW) by Solar TiO_2 Photocatalysis and Solar Photo-Fenton, *Solarenergy*, **77:** 567-572 (2004).

[16] Michael I., Panagi A., Ioannou L.A., Frontistis Z., Fatta-Kassinos D., Utilizing Solar Energy for the Purification of Olive Mill Wastewater Using a Pilot-Scale Photocatalytic Reactor after Coagulation-Flocculation, *Water Research*, **60(2):** 28-40 (2014)

[17] Fasihnia S.H., Peighambardoust S.H., Peighambardoust S.J., Oromiehie A., Soltanzadeh M., Peressini D., Migration Analysis, Antioxidant, and Mechanical Characterization of Polypropylene-based Active Food Packaging Films Loaded with BHA, BHT, and TBHQ *Journal of Food Science*, **85(8):** 2317-2328 (2020).

[18] Erdem S., Can Yarımtepe C., Ayman Öz N., Zeytin Karasuyunun Arıtım Yöntemleri, *Çanakkale onsekiz Mart Üniversitesi Fen Bilimleri Enstitüsü Dergisi*, **1:** 81-110 (2015)

[19] Justino C., Marques A.G., Duarte K.R., Duarte A.C., Pereira R., Rocha-Santos T., Freitas A.C., Degradation of Phenols in Olive Oil Mill Wastewater by Biological, Enzymatic and Photo-Fenton Oxidation, *Environ Sci Pollut Res*., **17(3):** 650-656 (2010).

[20] Shi J.W., Zheng J.T., Ji X.J., TiO_2-SiO_2/Activated Carbon Fibers Photocatalyst: Preparation, Characterization, and Photocatalytic Activity, *Environ. Eng. Sci.*, **27:** 923-930 (2010).

[21] Kumar S.G., Devi L.G., Review on Modified TiO_2 Photocatalysis Under UV/Visible Light: Selected Results and Related Mechanisms on Interfacial Charge Carrier Transfer Dynamics, *J. Phys. Chem. A.*, **115:** 13211-13241 (2011)

[22] Zhang C., Jiang Y., Li Y., Hu Z., Zhou L., Zhou M., Three-Dimensional Electrochemical Process for Wastewater Treatment: A General Review, *Chemical Engineering Journal*, **228:** 455-467 (2013).

[23] Kaur S., Singh V., Visible Light Induced Sonophotocatalytic Degradation of Reactive Red Dye 198 Using Dye Sensitized TiO_2, *Ultrasonics Sonochemistry*, **14(5):** 531–537 (2007)

[24] Uğurlu M., Vaizogullar A.I., Yilmaz I., Gunbeldek M., Chaudhary A.J., Electrocatalytic Oxidation of Reactive Orange 122 in Wastewater by Using Three-Dimensional Electrochemical Reactor (3DER), *Journal of the Chemical Society of Pakistan*, **40(3):** 475 (2018).

[25] Fil B.A., Boncukoğlu R., Yılmaz A.E., Bayar S., Antep Fıstığı İşleme Atıksularının Elektrooksidasyon Yöntemiyle on Arıtım Çalışmaları, *Iğdır Üni. Fen Bilimleri Enst. Der. / Iğdır Univ. J. inst. Sci. & Tech.,* **2(2):** 29-36 (2012*)*

[26] Akram N., Ma W., Guo J., Guo Y., Yansong Z., Hassan A., Wang J., Synergistic Catalysis of Fe_3O_4/CuO Bimetallic Catalyst Derived from Prussian Blue Analogues for the Efficient Decomposition of Various Organic Pollutants, *Chemical Physics,* **540:** 110974 (2021).

[27] AWWA (American Water Works Association), "American Public Health Association, American Water Works Association, Water Environment Federation", *Standard Methods for the Examination of Water and Wastewater, 23rd Edition,* 1368, (2017),

[28] Mahata S., Mondal B., Mahata S.S., Usha K., Mandal N., Mukherjee K., Chemical Modification of Titanium İsopropoxide for Producing Stable Dispersion of Titania Nano-Particles, *Materials Chemistry and Physics,* **151:** 267-274 (2015)

[29] Uğurlu M., Gürses A., Doğar C., Yalçın M., The Removal of Lignin and Phenol From Paper Mill Effluents By Electrocoagulation, *Journal of Environmental Management,* **87:** 420-428 (2008)

[30] Uğurlu M., Kula İ., Decolourization and Removal of Some Organic Compounds from Olive Mill Wastewater by Advanced Oxidation Processes and Lime Treatment, *Environmental Science and Pollution Research,* **14(5):** 319-25 (2007)

[31] Peighambardoust S.J., Pourabbas B., Preparation and Characterization of Nylon-6/PPy/MMT Composite of Nanocomposite, *Journal of Applied Polymer Science,* **106(1):** 697-705 (2007).

[32] Panahi F.H., Peighambardoust S.J., Davaran S., Salehi R., Development and Characterization of PLA-mPEG Copolymer Containing Iron Nanoparticle-Coated Carbon Nano-Tubes for Controlled Delivery of Docetaxel, *Polymer,* **117:** 117-131 (2017).

[33] Foroutan R., Peighambardoust S.J., Mohammadi R., Peighambardoust S.H., Ramavandi B., Development of New Magnetic Adsorbent of Walnut Shell Ash/Starch/Fe_3O_4 for Effective Copper Ions Removal: Treatment of Groundwater Samples, *Chemosphere,* **296:** 133978 (2022).

[34] Najafi A., A Novel Synthesis Method of Hierarchical Mesoporous MgO Nanoflakes Employing Carbon Nanoparticles as the Hard Templates for Photocatalytic Degradation, *Ceramics International,* **43(7):** 5813-5818 (2017)

[35] Mirgorod Y., Emelianov S., Fedosjuk V., Bolshanina S., Influence of Size Effects on the Properties of Processed Iron ore and Schungite Rock, *Journal of Nano-and Electronic Physics,* **8(2):** 2053 (2016).

[36] Uğurlu M., Karaoğlu H., Removal of AOX, Total Nitrogen and Chlorinated Lignin from Bleached Kraft Mill Effluents by UV Oxidation in the Presence of Hydrogen Peroxide Utilizing TiO_2 as a Photocatalyst, *Environ Sci Pollut Res.,* **16:** 265-273 (2009).

[37] Yu S.Q., Ling Y.H., Wang R.G., Zhang J., Qin F., Zhang Z.J., Constructing Superhydrophobic WO_3@TiO_2 Nanoflake Surface Beyond Amorphous Alloy Against Electrochemical Corrosion on İron Steel, *Applied Surface Science,* **436:** 527-535 (2018).

[38] Savari A., Hashemi S., Arfaeinia S., Dobaradaran S., Foroutan R., Mahvi A.H., Fouladvand M., Sorial G.A., Farjadfard S., Ramavandi B., Physicochemical Characteristics and Mechanism of Fluoride Removal Using Powdered Zeolite-Zirconium in Modes of Pulsed & Continuous Sonication and Stirring, *Advanced Powder Technology,* **31(8):** 3521-3532 (2020).

[39] Najafi A., A Novel Synthesis Method of Hierarchical Mesoporous MgO Nanoflakes Employing Carbon Nanoparticles as the Hard Templates for Photocatalytic Degradation, *Ceramics International,* **43(7):** 5813-5818 (2017).

[40] Choi S., Lee M.S., Park D.W., Photocatalytic Performance of TiO_2/V_2O_5 Nanocomposite Powder Prepared by Dc Arc Plasma, *Current Applied Physics,* **14(3):** 433-438 (231014).

[41] Karuppasamy K.M., Subrahmanyam A., The Electrochromic and Photocatalytic Properties of Electron Beam Evaporated Vanadium-Doped Tungsten Oxide Thin Films, *Solar Energy Materials and Solar Cells,* **92(11):** 1322-1326 (2008).

[42] Foo K.Y., Hameed B.H. A Short Review of Activated Carbon Assisted Electrosorption Process: An Overview. Current Stage and Future Prospects, *J. Hazard. Mater.,* **170:** 552-559 (2009).

[43] Huang C.C., Su Y.J., Removal of Copper İons from Wastewater by Adsorption/Electrosorption on Modified Activated Carbon Cloths, *J. Hazard. Mater.*, **175:** 477-483 (2010).

[44] Bán A., Schäfer A., Wendt H., Fundamentals of Electrosorption on Activated Carbon for Cwastewater Treatment of Industrial Effluents, *J. Appl. Electrochem.*, **28:** 227-236 (1998).

[45] Wang C.T., Chou W.L., Kuo Y.M., Chang F.L., Paired Removal of Color and COD From Textile Dyeing Wastewater By Simultaneous Anodic and indirect Cathodic Oxidation, *J. Hazard. Mater.*, **169(1-3):** 16-22 (2009).

[46] Piya-Areetham P., Shenchunthichai K., Hunsom M., Application of Electrooxidation Process for Treating Concentrated Wastewater from Distillery Industry with a Voluminous Electrode, *Water Res.*, **40:** 2857-2864 (2006).

[47] Wang C.T., Hu J.L., Chou W.L., Kuo Y.M., Removal of Color From Real Dyeing Wastewater By Electro-Fenton Technology Using A Three-Dimensional Graphite Cathode, *J. Hazard. Mater.*, **152(2):** 601-606 (2008).

[48] Wang B., Kong W., Ma H., Electrochemical Treatment of Papermill Wastewater Using Three-Dimensional Electrodes with Ti/Co/SnO_2–Sb_2O_5 Anode, *J. Hazard. Mater.*, **146(1-2):** 295-301 (2007).

[49] Yan L., Ma H., Wang B., Wang Y., Chen Y., Electrochemical Treatment of Petroleum Refinery Wastewater with Three-Dimensional Multi-Phase Electrode, *Desalination*, **276(1-3):** 397-402 (2011).

[50] Zhou M., Lei L., The Role of Activated Carbon on the Removal of Para-Nitrophenol in an Integrated Three-Phase Electrochemical Reactor, *Chemosphere*, **65:** 1197-1203 (2006).

[51] Shen B., Wen X., Huang X., Enhanced Removal Performance of Estriol by a Three-Dimensional Electrode Reactor, *Chemical Engineering Journal*, **327:** 597-607 (2017).

[52] Sonkara M., Kumar M., Dutta D., Kumar V., Treatment of Pulp and Paper Mill Effluent by a Novel Bacterium Bacillus sp. IITRDVM-5 through a Sequential Batch Process, *Biocatalysis and Agricultural Biotechnology*, **20:** 101232 (2019).

[53] Fortuny A., Font J., Fabregat A., Wet Air Oxidation of Phenol Using Active Carbon as Catalyst, *Appl. Catal. B.*, **19(3-4):** 165-173 (1998).

[54] Huang B-.R., Lin J-.C., Lin T-.C., Mangindaan D., Wang M-.J., The Effect of Tetrafluoromethane Plasma Post-Treatment on the Electrical Property of Tungsten Oxide Nanowires, *J. Nanosci. Nanotechnol.*, **11(9):** 7693-7699 (2011).

[55] Zhu L., Meng Z., Park C., Ghosh T., Oh W., Characterization and Relative Sonocatalytic Efficiencies of A New Mwcnt and Cds Modified TiO_2 Catalysts and their Application in the Sonocatalytic Degradation of Rhodamine B, *Ultrasonics Sonochemistry*, **20(1):** 478-484 (2013).

[56] Lv G., Wu D., Fu R., Performance of Carbon Aerogels Particle Electrodes for the Aqueous Phase Electro-Catalytic Oxidation of Simulated Phenol Wastewaters, *J. Hazard. Mater.*, **165(1-3):** 961-966 (2009).

[57] Toczyłowska-Mamińska R., Limits and Perspectives of Pulp and Paper Industry Wastewater Treatment, A Review, *Renewable and Sustainable Energy Reviews*, **78:** 764-772 (2017)

[58] Yang Y., Recent Advances in the Electrochemical Oxidation Water Treatment: Spotlight on Byproduct Control, *Frontiers of Environmental Science & Engineering* **14**: 85 (2020).